A Comparison of Fabrication Precision and Mechanical Reliability of 2 Zirconia Implant Abutments

Robert B. Kerstein, DMD[1]/John Radke, BA, MBA[2]

Purpose: *Studies have described the reliability of zirconia as an implant abutment material. The purpose of this in vitro study was to compare the precision and fracture strength of 2 different zirconia abutments angled at 30 degrees and loaded to failure in a standardized testing device.* ***Materials and Methods:*** *Twenty-nine Atlantis abutments in zirconia (AAZ) and 29 Nobel Biocare Procera AllZirkon abutments of comparable interface were measured for key interface feature statistical differences (analysis of variance; α = 95%). Each specimen was fixed to a regular-platform Brånemark System implant and mounted in an Instron machine. Increasing incremental loads were applied until failure. A 2-tailed* t *test for independent specimens and unequal variances was employed (α = 95%). The Weibull method determined the probability of failure of each abutment sample (α = 95%). Fractography by scanning electron microscopy determined the flaws at the fracture origins.* ***Results:*** *Metrology inspection indicated that the AAZ showed no measurable dimensional differences of 4 key interface features. The mean failure load of the AAZ (831 N) was greater than the AllZirkon (740 N;* P *<.00006). The Weibull distribution showed that the AAZ would be more likely to survive intraoral occlusal loads (*P *< .0005).* ***Conclusions:*** *Both types of zirconia abutments demonstrated failure loads that exceed maximum human bite force. In vitro, the AAZ outperformed the AllZirkon in survivability. The clinical use of zirconia abutments is indicated when esthetics may be of concern.* Int J Oral Maxillofac Implants 2008;23:1029–1036

Key words: *fractography, fracture strength, key interface features, metrology inspection, Weibull modulus*

The current state of the art in esthetic implant prosthodontics is employing all-ceramic crowns with all-ceramic abutments to optimize the esthetics of anterior tooth replacements. All-ceramic abutments were previously made from pressed and sintered aluminum oxide. Clinical survival studies[1,2] of all-ceramic abutments have shown that these nonmetallic abutments demonstrate adequate short-term intraoral durability. In one study over a 3-year period of observation, 43 of 44 all-ceramic abutments functioned intraorally, with only 1 exhibiting fracture.[1]

In recent years, glass-infiltrated alumina and yttria-stabilized zirconium oxide abutments have been introduced.[3] Comparisons of aluminum oxide (or alumina) abutments and zirconium oxide (or zirconia) abutments revealed that both types of all-ceramic abutments exceeded the established values for maximum incisal forces reported in the literature (90 to 370 N).[4,5] Zirconia abutments were found to be more than twice as resistant to fracture as alumina abutments.[6]

Published studies indicate that zirconia can be used as an implant abutment material.[3,6–11] One study analyzed anterior zirconia, titanium, and aluminous porcelain test abutments that were artificially aged; the median fracture resistance of the zirconia abutments was 443.6 N. This load is very near the

[1]Formerly Assistant Clinical Professor, Department of Restorative Dentistry, Tufts University School of Dental Medicine, Boston, Massachusetts. Currently in private practice.
[2]President, BioResearch Associates. Inc., Milwaukee, Wisconsin.

Correspondence to: Dr Robert B. Kerstein, 665 Beacon St. #204, Boston, MA 02215. Fax: +617-247-1611. E-mail: tmjdoc@ix.netcom.com

Fig 1 Atlantis abutment in zirconia test sample (*left:* lateral view; *right:* interface).

Fig 2 Nobel Biocare Procera AllZirkon abutment test sample (*left:* lateral view; *right:* interface).

high end of human occlusal forces, indicating that zirconia has the potential to withstand physiologic occlusal forces applied in the anterior region.[7] Another study that also artificially aged the test specimens (zirconia crowns and implant abutments) showed again that zirconia, as a dental material, fractures at a high enough force to withstand maximum human occlusal loads.[8]

Despite the amount of existing data that indicates zirconia is strong enough to be used intraorally (at least anteriorly), standardized tests and appropriate methods of statistical analysis have not been performed to compare the strength of computer-designed zirconia abutments made by different manufacturing processes.

The purpose of this in vitro study was to compare 2 commercially available types of zirconia abutments: the Procera AllZirkon (Nobel Biocare Holding, Kloten, Switzerland), and the Atlantis abutment in zirconia (AAZ) (Atlantis Components, Cambridge, MA, USA). Both abutment systems use computer-aided technology to create their abutment contours. The Procera process scans a technician-created wax abutment from which a zirconia blank is computer milled to reproduce the technician-determined abutment shape. The Atlantis process scans the master cast to detect soft tissue contours, occlusal clearance, and implant location. A virtual abutment is then designed and optimized based upon parametric ideal abutment shapes with design constraints.[12] After the virtual design is completed, it is milled from a zirconia blank.

MATERIALS AND METHODS

Twenty-nine AAZ and 29 AllZirkon abutments were created by their respective manufacturers. The AAZ was created using proprietary computer design techniques, resulting in guided milling of the specific contours to replicate a maxillary central incisor (Fig 1). The AllZirkon abutment was waxed in a shape similar to the Atlantis abutment and manufactured using the Procera proprietary technique (Fig 2). All of the abutments were designed to fit a Nobel Biocare regular-platform, 4.0-mm-diameter, external-hex dental implant (Nobel Biocare Holding).

Table 1 Summary of Dimensional Characteristics of Key Interface Features

	AAZ	AllZirkon
Interface geometry	Nobel Biocare external-hex 4.0 mm	Nobel Biocare external-hex 4.0-mm
No. of specimens	10	10
Mean hex flat-to-flat (mean of 3 measurements of opposite hex walls [SD])	2.731 mm (0.004 mm)	2.758 mm (0.010 mm)
Mean bore diameter (SD)	2.138 mm (0.003 mm)	2.148 mm (0.012 mm)
Mean counterbore diameter (SD)	2.626 mm (0.009 mm)	2.673 mm (0.031 mm)
Mean true position of counterbore to bore (SD)	0.029 mm (0.010 mm)	0.075 mm (0.056 mm)

Table 2 ANOVA of Hex Dimensions

	Sum of squares	*df*	Mean square	F	*P*
Procera hex 1–4					
Between groups	.001	7	.000	1.970	.378
Within groups	.000	2	.000		
Total	.001	9			
Procera hex 2–5					
Between groups	.001	7	.000	.615	.737
Within groups	.000	2	.000		
Total	.001	9			
Procera hex 3–6					
Between groups	.001	7	.000	.678	.708
Within groups	.000	2	.000		
Total	.001	9			
AAZ hex 1–4					
Between groups	.001	7	.000	8.644	.108
Within groups	.000	2	.000		
Total	.001	9			
AAZ hex 2–5					
Between groups	.000	7	.000	.300	.904
Within groups	.000	2	.000		
Total	.000	9			
AAZ hex 3-6					
Between groups	.000	7	.000	.583	.753
Within groups	.000	2	.000		
Total	.000	9			

Table 3 Table 3 ANOVA of Bore Diameter Concentricity

	Sum of squares	*df*	Mean square	F	*P*
Procera					
Between groups	.001	7	.000	1.496	.458
Within groups	.000	2	.000		
Total	.001	9			
AAZ					
Between groups	.000	7	.000	.527	.780
Within groups	.000	2	.000		
Total	.000	9			

Table 4 ANOVA of Counterbore

	Sum of squares	*df*	Mean square	F	*P*
Procera					
Between groups	.007	6	.001	1.928	.315
Within groups	.002	3	.001		
Total	.009	9			
AAZ					
Between groups	.000	6	.000	.616	.720
Within groups	.000	3	.000		
Total	.001	9			

Prior to strength testing, 10 abutments of each type were randomly selected for metrology inspection. Dimensions of 4 key interface features for each of the 2 sample groups were determined using a coordinate measuring machine (CMM) (Brown and Sharpe, North Kingston, RI, USA) that had a 9 × 12 × 8-inch x,y,z measurement volume. Calibration of the unit was in accordance with ISO 10360-2 Part 2. The CMM employed a small-diameter touch probe to make point contact with each surface of the key abutment interface dimensions: hex flat to flat (3 measurements, 1 of each pair of opposing walls of the hex); counterbore to through bore; degree of bore concentricity; and true position of the through bore (Table 1). Statistical treatment of the metrology data of the 4 key interface features was accomplished with analysis of variance (ANOVA; Tables 2 to 5) (SPSS version 13.0 for Windows, SPSS, Chicago, IL, USA) ($\alpha = .05$).

Table 5 ANOVA of True Position of Bore to Counterbore

	Sum of squares	*df*	Mean square	F	*P*
Procera					
Between groups	.026	6	.004	7.087	.068
Within groups	.002	3	.001		
Total	.028	9			
AAZ					
Between groups	.001	6	.000	2.649	.227
Within groups	.000	3	.000		
Total	.001	9			

Fig 3 Zirconia abutment mounted in test apparatus at 40-degree angle to the applied load.

Table 6 Summary of Mechanical Reliability (Strength) and POF Data

Description	Atlantis AAZ (n = 29)	Procera AllZirkon (n = 29)
Sample geometry	Abutment geometry; FDA Guidance Document[13]	
Weibull distribution parameters		
Shape parameter	15.1 (11.6–19.7)	10.6 (7.9–14.1)
Scale parameter	858 N (837–880 N)	777 N (749–805 N)
POF estimates		
At 300 N	1 ppm	32 ppm
At 450 N	57 ppm	3,093 ppm
At 600 N	4,436 ppm	62,950 ppm

Each test specimen was designed to correct a 30-degree misalignment of the implant body. The implants were fixed at a 40-degree angle to the loading direction such that the abutment was undercorrected by 10 degrees, simulating maximum implant-abutment misalignment and off-axis loading. Each specimen was assembled to the test implant using each manufacturer's supplied screws and mounted rigidly into an Instron universal testing machine (Model 1122, Instron Corporation, Norwood, MA) (Fig 3), in accordance with test recommendations made by the United States Food and Drug Administration.[13]

The implants were clamped into place 3 mm below their abutment mating surface so that the implants' long axis made a 40-degree angle with the loading direction of the Instron machine loading frame**.** The screw of every assembly was torqued to Nobel Biocare's prescribed 35 Ncm. The Instron crosshead applied a load to the center of a sphere integrated into the abutment geometry, in a plane defined by the long axes of the implant and the abutment. The crosshead, once activated, moved toward the assembly at a continuous speed of 0.05 inches per minute until it contacted the test specimen. Loading started at 0 N and was increased until failure of the test specimen was induced.

The maximum failure load each sample reached was recorded. Means and standard deviations were calculated (Table 6). The F test showed that the 2 strength distributions were approximately normal; therefore a 1-tailed, independent-sample Student *t* test for equal variances was used to compare the means of the strength values of the 2 differing abutment types.

A power analysis was employed to determine whether the sample size of 29 specimens per group was large enough to correctly reject the null hypothesis that the mean fracture strength of the AAZ was significantly different than that of the AllZirkon (the alternative hypothesis would be no significant difference in fracture strength of the 2 samples). The power is $1 - \beta$, where β is the probability of that the null hypothesis is wrongly accepted. Because no standard fracture force was determined prior to testing, the larger mean value of the AAZ was used as the reference value ($\alpha = .05$) to calculate β. The lower bound of the rejection region is represented by the equation $X_L = 837 - 1.645\ (69.01/29^{1/2}) = 809.62$. Using the alternative mean (from the test of AllZirkon) and the weighted average of the 2 standard deviations, $z = (U_0 - U_A)/83.4 = 1.09$. Substituting for β: $\beta = 0.5 - 0.3621 = 0.1379$. The power of this study therefore equaled $(1 - 0.1379) = 86\%$, such that for the number of specimens tested per group (29), 86% of the time the null hypothesis would be rejected if it was untrue.

An evaluation of the probabilities of failure (POF) was evaluated in accordance with ASTM 1239-06.[14] This standard provides guidelines for estimating the brittle failure probability distribution parameters for advanced ceramic materials. The 95% confidence bounds of the Weibull distribution parameters (Figs 4 and 5) were calculated using the maximum likeli-

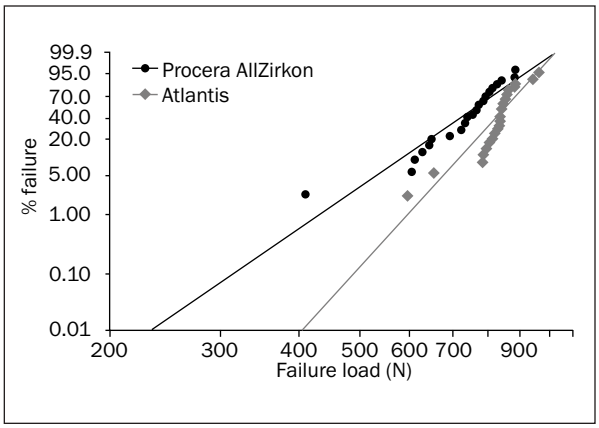

Fig 4 Weibull probability plot for failure load of abutments.

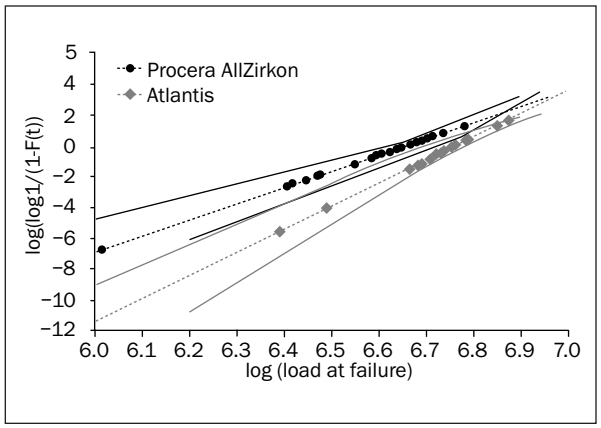

Fig 5 Weibull maximum likelihood estimate plot for failure load of abutments.

Fig 6 *(left)* SEM image of fracture surface of AAZ (magnification ×20).

Fig 7 *(Right)* Higher magnification of fracture surface of AAZ (magnification ×100).

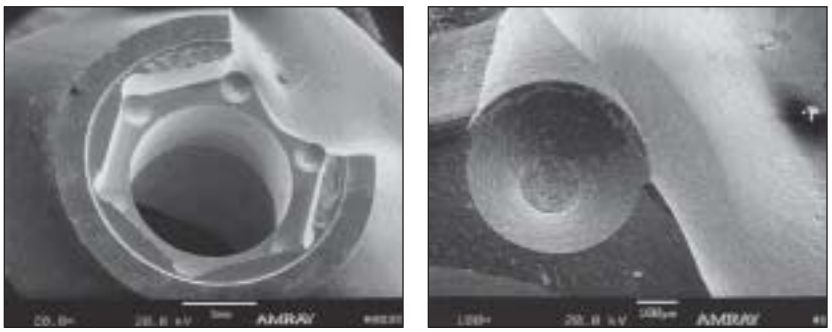

Fig 8 *(left)* SEM image of fracture surface of Procera AllZirkon abutment (magnification ×24).

Fig 9 *(Right)* Higher magnification of fracture surface of Procera AllZirkon abutment (magnification ×100).

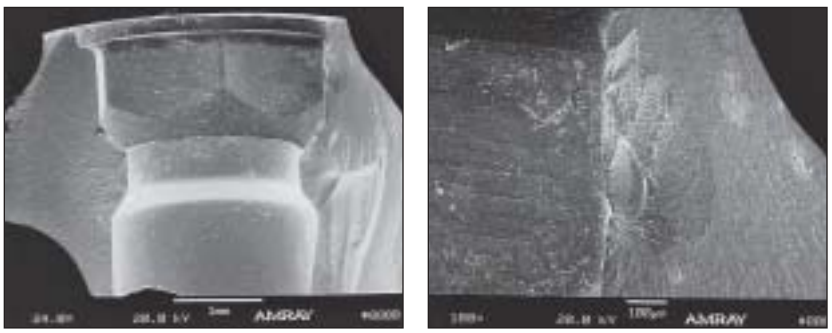

hood estimation technique, assuming all failures originated from a single flaw population of uncensored specimens. All strength data observations were used in the analysis, as no specimen was excluded.

Finally, fractographic analyses were conducted to determine the location and nature of the fracture origins (Figs 6 to 9). This postfailure analysis was conducted using a combination of optical microscopy and scanning electron microscopy (SEM) (Amray model #1830I, Amray Mfg, Bedford, MA, USA).

RESULTS

Abutment Metrology

The ANOVA performed on the metrology data of the 4 key interface features (hex dimensions, Table 2; bore diameter concentricity, Table 3; diameters of the counterbores, Table 4; true position of the bore to the counterbore, Table 5) determined that each of these key interface features of the 2 differing abutment designs were not significantly different.

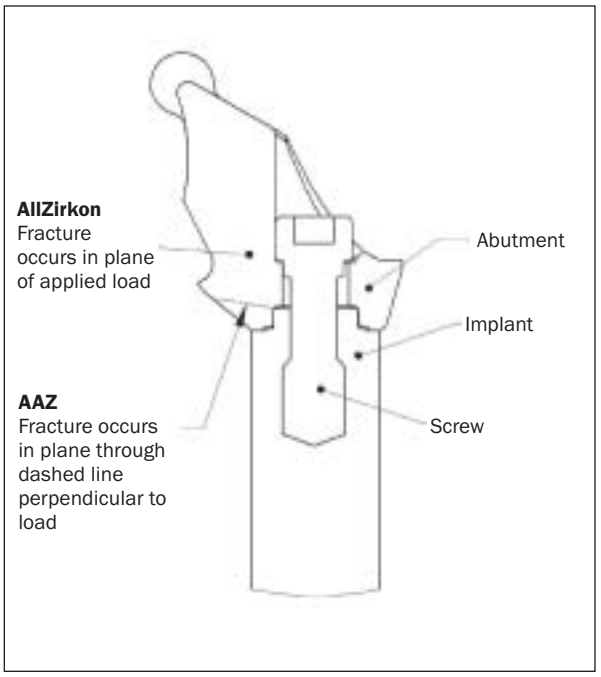

Fig 10 Fracture locations on both abutments.

Abutment Mechanical Reliability

The mean failure load of the AAZ abutments was 831 ± 69 N, whereas the failure load of the AllZirkon abutments was 740 ± 96 N. This was a statistically significant difference ($P < .00006$). The load to failure data are provided in Table 6.

Probability of Abutment Failure

The Weibull distribution is a continuous probability distribution with the probability density function

$$f(x; k, \lambda) = {}^{k}\!/\!_{\lambda}({}^{x}\!/\!_{\lambda})^{k-1} e^{-({}^{x}\!/\!_{\lambda})^{k}}$$

for $x \geq 0$ and $f(x; k, \lambda) = 0$ for $x < 0$, where $k > 0$ is the shape parameter (slope of the Weibull Distribution) and $\lambda > 0$ is the scale parameter of the distribution.

The cumulative distribution function is:

$$F(x; k, \lambda) = 1\text{-}e^{-({}^{k}\!/\!_{\lambda})^{k}}$$

for $x \geq 0$, and $F(x; k; \lambda) = 0$ for $x < 0$.

The failure rate h (or hazard rate) is given by the equation

$$h(x; k, \lambda) = {}^{k}\!/\!_{\lambda}({}^{x}\!/\!_{\lambda})^{k-1}$$

This describes the likelihood of abutment survival when subjected to increasing loads. For this study it was assumed that the populations of failure strengths were representative of a 2-parameter (slope and scale) Weibull distribution.

Figures 4 and 5 illustrate the load at failure data and the POF rates for the 2 samples of zirconia abutments in Weibull probability graphic format. At loads in line with human bite loads,[4,5] the AllZirkon abutment demonstrated a higher POF than the AAZ abutment under the same loading conditions (Table 6).

Fractographic Analysis

SEM analysis at 2 differing magnifications showed that failure origins from both abutment types were typically small irregularities in the as-processed surface, with one exception from the population of AllZirkon specimens. Most of these surface irregularities were so small (on the order of the size of the zirconia grains) that the specific flaw at the failure origin could not be identified. No flaws or voids were detected in the fractured surfaces (with 1 AllZirkon exception).

Typical fractured surfaces for the AAZ and the AllZirkon test abutments can be seen in the SEM photomicrographs (Figs 6 to 9). The arrows indicate the approximate failure origin sites, as determined by visual inspection of the SEM photomicrograph. A detailed diagram that illustrates the fracture origins for both abutment types is provided in Fig 10.

The fractography revealed noticeable differences in the crack propagation between the AAZ and the AllZirkon. The AAZ exhibited consistent fracture origin of the inner-hex interface surfaces of all test abutments (Figs 6, 7, and 10). The magnified fractured surface appears smooth and continuous throughout the fractured surface. The mirror and mist of the fracture extend out from the initiation site uniformly. Both of these regions appear smooth. In the hackle region there are a few visible hackle lines present, with a minimum of branching (Fig 7).

The AllZirkon exhibited fracture origin at the radius inside the hexagon interface feature (Figs 8 to 10). The magnified fractured surface appears visibly uneven. The mirror is clearly surrounded by the mist, which extends out in a nonuniform manner from the initiation site. The mist is surrounded by numerous uneven raised regions within the mirror. Throughout the hackle region there are numerous visible hackle lines, which demonstrate significant branching (Fig 9).

DISCUSSION

The results of this study are comparable to previous studies of zirconia abutments,[3,6–11] conducted in

non–Food and Drug Administration designed test conditions, showing that both the AAZ and the AllZirkon abutments can withstand human occlusal loads. However, in this study the AAZ demonstrated statistically significant higher strength values than did the AllZirkon abutments, as well as a lower POF.

Metrologic inspection of the 2 populations of zirconia abutments revealed no significant differences between the interface features measured. Therefore, their respective significant strength difference would most probably not be related to the precision of their respective fabrication processes, but more likely was a result of the raw stock zirconia material that each company uses in its abutment fabrication process.

Clinical survivability of ceramic materials depends on their ability to withstand intraoral forces. In this study, no cyclic loading to simulate aging prior to testing was employed. Prior published artificial aging studies showed that the aging process did not significantly affect the fracture strength of the zirconia test specimens.[7,8] In this study, abutment strength and survivability were determined by applying an increasing load until failure occurred. This method evaluated the absolute strength characteristics of the 2 differing abutment materials.

The greater fracture strength of the AAZ is reflected in the POF data seen in Figs 4 and 5. Graph representations of the Weibull distribution fit parameters illustrate the Weibull modulus (m value) as the slope of the linear fit of the load to failure data. A higher slope of the m value indicates less statistical variation of the load to failure data and translates into a lower POF at lower loads (the left side of the Weibull plots). One can interpret this graph representation by determining the failure probability at a given load. At a reference load of 600 N (30% greater than the estimated maximum human bite load), the probability of survival for the AAZ was 0.996, or a POF of 4 parts in 1,000. The POF for the AllZirkon was 0.932, or a failure probability of 68 parts in 1,000. The calculations of POF at loads in line with human bite loads requires expression in parts per million (ppm). For AAZ at 300 N (median human bite load), the POF = 1 ppm; at 450 N, the POF = 57 ppm; and at 600 N, the POF = 4,436 ppm. For the AllZirkon, the POF value at 300 N = 42 ppm; at 450 N (moderately strong human bite load), the POF = 3,093 ppm; and at 600 N, the POF = 62,950 ppm. The AAZ demonstrated a higher probability of survival at varying intraoral loads. Figure 5 shows the same load at failure data for the 2 populations of zirconia abutments in the graph format by estimating the shape and scale of the Weibull distribution fit parameters using the maximum likelihood method. The dashed lines represent the Weibull distributions based on the estimated nominal fit parameters. The solid lines represent the 95% confidence boundaries of the maximum likelihood fit estimates for Weibull modulus (shape factor) and characteristic strength (scale factor) for each population. These 2 confidence boundary zones for the most part do not overlap, indicating that the differences in Weibull modulus and characteristic strengths between the 2 populations are statistically significant. The Weibull modulus data are summarized in Table 6.

A limitation of this study was that the AllZirkon abutment was waxed into a shape similar to the original computer-designed Atlantis abutment. Therefore the shapes and dimensions of the 2 test abutment designs were not identical, which could possibly affect the fracture strength results. It would have been more ideal to have the waxed AllZirkon design scanned into the Atlantis software, from which the AAZ could have been created. This would have then made the 2 differing test abutments dimensionally identical.

CONCLUSION

Fifty-eight zirconia abutments developed by 2 different manufacturers were preliminarily measured for their precision of key abutment interface features and then tested with increasing constant load until fracture. There were no significant differences between the 4 key interface features measured on the 2 differing abutment samples. However, the mean load to failure for the Atlantis abutment in zirconia was significantly higher than that of the AllZirkon abutment, and the Atlantis abutment demonstrated a statistically significant lower probability of failure across the range of human occlusal loads. Fractography conducted after fracture revealed visible differences in the initiation location and crack propagation between the 2 differing test abutments. Since both abutment types demonstrated failure loads that exceed the studied values of maximum human bite force, their clinical use is indicated as an alternative to titanium and/or cast metal abutments when esthetics may be of concern.

ACKNOWLEDGMENTS

The lead author is a clinical consultant for Atlantis Components, Inc. He will receive no compensation for the publication of this manuscript. Funding for this study was provided by Atlantis Components, Cambridge, Massachusetts.

REFERENCES

1. Andersson B, Taylor A, Lang BR, et al. Alumina ceramic implant abutments used for single-tooth replacement: A prospective 1- to 3-year multicenter study. Int J Prosthodont 2001;14: 432–438.
2. Andersson B, Scharer P, Simion M, Bergstrom C. Ceramic abutments used for short-span fixed partial dentures: A prospective 2-year multicenter study. Int J Prosthodont 1999;12: 318–324.
3. McLaren EA, White SN. Glass-infiltrated zirconia alumina-based ceramic for crowns and fixed partial dentures. Pract Periodontics Aesthet Dent 1999;11:985–994.
4. Lyons MF, Cadden SW, Baxendale RH, Yemm R. Twitch interpolation in the assessment of the maximum force-generating capacity of the jaw-closing muscles in man. Arch Oral Biol 1996;41:1161–1168.
5. Proeschel PA, Morneburg T. Task-dependence of activity/bite-force relations and its impact on estimation of chewing force from EMG. J Dent Res 2002;81:464–468.
6. Yildirim M, Fischer H, Marx R, Edelhoff D. In vivo fracture resistance of implant-supported all-ceramic restorations. J Prosthet Dent 2003;90:325–331.
7. Att W, Kurun S, Gerds T, Strub JR. Fracture resistance of single-tooth implant-supported all-ceramic restorations: An in vitro study. J Prosthet Dent 2006 Feb;95(2):111–116.
8. Kohal RJ, Klaus G, Strub JR. Zirconia-implant-supported all-ceramic crowns withstand long-term load: A pilot investigation. Clin Oral Implants Res 2006 Oct;17(5):565–571.
9. Prestipino V, Ingber A. Esthetic high-strength implant abutments. Part I. J Esthet Dent 1993;5:29–36.
10. Prestipino V, Ingber A. Esthetic high-strength implant abutments. Part II. J Esthet Dent 1993;5:63–68.
11. Glauser R, Sailer I, Wohlwend A, Studer S, Schibli M, Schärer P. Experimental zirconia abutments for implant-supported single-tooth restorations in esthetically demanding regions: 4-year results of a prospective clinical study. Int J Prosthodont 2004;17:285–290.
12. Kerstein RB, Castellucci F, Osorio J. Utilizing computer generated titanium permanent healing abutments to promote ideal gingival form and anatomic restorations on implants. Compend Contin Educ Dent 2000;21:793–802.
13. Class II Special Controls Guidance Document: Root-form Endosseous Dental Implants and Endosseous Dental Abutments. U.S. Food and Drug Administration, Section 8 Mechanical Properties, May 14, 2002. [AU: Place of publication?]
14. Standard Practice for Reporting Uniaxial Strength Data and Estimating Weibull Distribution Parameters for Advanced Ceramics. ASTM 1239-06. West Conshohocken, PA: ASTM International.